Contribution of different parameters to the thrust deduction of a waterjet propelled hull

CONTRIBUTION OF DIFFERENT PARAMETERS TO THE THRUST DEDUCTION OF A WATERJET PROPELLED HULL

A. Eslamdoost, L. Larsson, R. Bensow
Department of Shipping and Marine Technology, Chalmers University of Technology, 412 96 Gothenburg, Sweden

SUMMARY
In order to model the waterjet-hull interaction a method, which is based on the potential flow assumption with non-linear free surface boundary conditions, is developed and validated. By means of this method the effect of the sinkage, trim and local flow variation on the resistance increment of a waterjet driven craft has been estimated. Besides, assuming that each of the aforementioned parameters independently influences the resistance change, the resistance increment of the hull is estimated through a linear expansion in a Taylor series, which is a function of the hull sinkage, trim and the flow rate through the waterjet unit. Knowing the magnitude of each single parameter separately helps to understand the physics behind the thrust deduction and may aid in the optimization of the hull/propulsor configuration. Also it sheds some light on the reason for the negative thrust deduction fractions sometimes found on waterjet driven hulls.

1. INTRODUCTION

Waterjet propulsion systems are frequently used for high-speed vehicles, particularly on craft, which require high manoeuvrability. The key point in the operation of waterjet systems is the momentum increment of the water drawn through a ducting channel by the action of an internal pump. The difference between the low momentum flow at the system intake and high-momentum flow expelled out of the nozzle generates the required thrust force for propelling the craft.

The objective of the present research is to study the interaction between the waterjet unit and the hull. While propeller-driven hulls always have a larger resistance than the corresponding towed hull, hence a positive thrust deduction factor, waterjet-driven hulls may well have a negative thrust deduction [1]. This does not necessarily mean that the waterjet hull has a lower resistance than the bare hull, since the definition of the thrust deduction factor is slightly different from that of conventional propeller hulls. In this paper, first a newly developed method for modelling waterjet-driven vessels based on the potential flow assumption with non-linear free surface boundary conditions is introduced and then, employing this method, the different components contributing to the thrust deduction for a waterjet-driven hull are investigated.

1.1. GENERAL DEFINITIONS

In this section, general definitions such as the control volume, thrust and thrust deduction fraction of a waterjet unit are discussed. Figure 1 shows the cross section of a waterjet propulsion unit and the control volume, which is normally applied for the system analysis. The numbering of the surfaces shown in Figure 1 is the same as those introduced by van Terwisga [1]. Some other possible control volumes are also described in [1].
Surface 1 is named capture area and is positioned one intake width ahead of the intake ramp tangency point. Avoiding the major flow distortions caused by the intake geometry is the reason for selecting the position of the capture area ([2], [3]). Surface 2 in Figure 1 shows the dividing streamtube. This streamtube is an imaginary surface, which separates the flow drawn into the ducting system from the rest of the flow field. According to the definition of a streamtube, no flow crosses this surface. Surface 4 is the outer-lip surface and surface 6 shows the waterjet system internal material boundaries. Surface 7 is the boundary area of the pump control volume and surface 8 represents the nozzle discharge area.

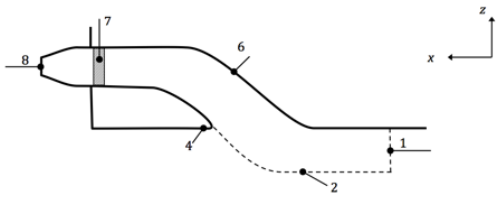

Figure 1. Section cut through the waterjet ducting system

Considering the introduced control volume, the net and the gross thrust of a waterjet unit can be defined. The gross thrust, $\vec{T}_g$, is defined as "the force vector pertinent to the change in momentum flux over the selected control volume, acting on its environment" [1]. The gross thrust is a vector, but since only the horizontal component of this vector, $T_{g,x}$, will be of interest in the following, for simplicity it will be referred to as the gross thrust, T_g .

$$T_g = -\iint_{A_1+A_8} \rho u_x (u_k n_k) dA \qquad (1)$$

where ρ is the density of the fluid, u is the velocity vector and *n* is the unit vector normal to the control volume surface.
Considering the material boundaries of the waterjet system, another thrust force may be defined. "The net thrust, $\vec{T}_{net}$, is defined as the force vector acting upon the material boundaries of the waterjet system, directly passing the force through to the hull" [1]. In the following, the horizontal component of the net thrust

vector will be called the net thrust, T_{net}, which is defined as ,

$$T_{net} = -\iint_{A_4+A_6} \sigma_x dA - \iiint_{V_7} \rho F_{px} dV \quad (2)$$

where σ_x and F_{px} are the horizontal components of the stresses acting on the control volume and the pump force, respectively.

For a conventional propeller, the thrust deduction relates the resistance of the bare hull to the net thrust required for driving the hull at a certain Froude number; but due to technical issues, it is not easy to measure the net thrust of the waterjet system, so the gross thrust is normally employed in the definition of the total thrust deduction fraction, *t*

$$T_g(1-t) = R_{bh} \quad (3)$$

where R_{bh} is the bare hull resistance.

In order to relate the net thrust to the gross thrust, a jet system thrust deduction fraction is defined from

$$T_{net} = T_g(1-t_j) \quad (4)$$

The total thrust deduction fraction, t, contains both the jet system thrust deduction, t_j and a thrust deduction fraction, t_r defined by the hull resistance increment, r. The latter thrust deduction is the one normally employed in conventional propeller/hull theory and is defined as follows:

$$T_{net}(1-t_r) = R_{bh} \quad (5)$$

Combining Equations (3), (4) and (5) and neglecting the second order terms, it is seen that the total thrust deduction, t, is equal to the sum of the thrust deduction due to the resistance increment, t_r, and the jet system thrust deduction t_j:

$$t = t_r + t_j. \quad (6)$$

2. PRESSURE JUMP METHOD

Generally, the duty of the waterjet pump is to increase the total head of the flow. The rise of the flow head, which occurs when the water passes through the impeller, might be interpreted as an abrupt pressure rise, here referred to as the pressure jump. The pressure jump is the fundamental concept behind the developed method for modelling the waterjet propulsion system and, therefore, this approach is called the Pressure Jump Method. The following sections describe the theory behind this method, its mathematical formulation and combination with a potential flow solver. The more common expression "actuator disk" is not used, since there is no such disk present in the actual implementation of the method, as will be explained below.

2.1. FORMULATION

To start with, the force balance for the waterjet-hull system must be formulated. The contribution of different parts of the system to the total resistance is depicted in Figure 2. In this figure, R_H is the hull resistance, R_D is the ducting channel drag excluding that of the nozzle chamber and R_N is the drag of the nozzle chamber. F_p is the force exerted by the impeller.

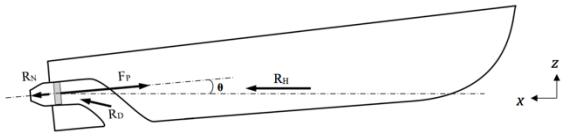

Figure 2. Force balance of the waterjet-hull system

Writing the force balance in the *x*-direction for the system in Figure 2, results in

$$F_{P,x} = R_H + R_{D,x} + R_{N,x} \quad (7)$$

Because of the action of the pump, there is a difference in pressure between the sides of the impeller. In fact, this pressure jump at the impeller section is the main source of the created thrust force of the waterjet system.

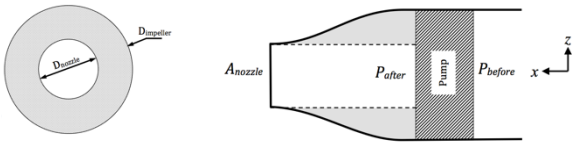

Figure 3. Schematic presentation of the nozzle section

A simplified sketch of the nozzle geometry is shown in Figure 3. The right hand side sketch in this figure shows a section cut of the nozzle and the left hand side sketch shows the perspective of the nozzle normal to its axis. Comparing two cases with the same nozzle exit velocity, one with and one without the pressure jump, the total head increase will result in a constant increase in static pressure in the nozzle. This is so, since the flow velocity will be unchanged. There will be no contribution to the thrust from the pressure increase inside the grey zone (Figure 3) since it is cancelled out internally. Then the only remaining high pressure zone which can create thrust will be the pressure acting on the perspective of the nozzle opening on the impeller disk. Setting this thrust force equal to the resistance of the entire system yields:

$$\Delta p \cdot A_{nozzle} \cdot \cos\theta = F_{P,x} = R_H + R_{D,x} + R_{N,x} \quad (8)$$

where, Δp indicates the pressure difference between two sides of the impeller and A_{nozzle} is the opening area of the nozzle and is multiplied by the cosine of the nozzle exit inclination angle with respect to the horizontal plane, θ, to extract the horizontal component of the thrust force. A more detailed mathematical derivation of the pressure jump equation (Equation (8)) can be found in [4].

2.2. POTENTIAL FLOW ASSUMPTION

The following assumes that the flow from the capture area to the nozzle exit is inviscid and, therefore, there is no head loss inside the ducting channel. In other words, the total head at section 8 becomes equal to the total head at section 1 (see Figure 1) plus the pressure jump, Δp. This is expressed through Bernoulli's equation in Equation (9). The pressure at the nozzle outlet section is assumed to be atmospheric. Subscripts applied in

Equation (9) are based on the notation presented in Figure 1;

$$\left[\bar{p}_1 + \rho g\bar{h}_1 + \frac{1}{2}\rho\overline{u_1^2}\right] + \Delta p = \bar{p}_{atm} + \rho g\bar{h}_8 + \frac{1}{2}\rho\overline{u_8^2} \qquad (9)$$

where ρ is the water density and g is the gravitational acceleration. $\bar{p}_1$ and $\bar{p}_{atm}$ represent the average pressures at the capture area and atmospheric pressure, respectively. The average heights of the capture area and nozzle outlet section are denoted by $\bar{h}_1$ and $\bar{h}_8$, respectively. $\bar{u}$ and $\bar{u}_8$ represent the average velocities at sections 1 and 8.

All terms in Equation (9) are known except the term containing the jet velocity, $\bar{u}_8$. By rearranging the equation for obtaining $\bar{u}_8$ and then dividing both sides by the undisturbed velocity, u_∞, the following equation emerges.

$$\frac{\bar{u}_8}{u_\infty} = \pm\sqrt{\frac{(\bar{p}_1 - \bar{p}_{atm})}{\frac{1}{2}\rho u_\infty^2} + \frac{\Delta p}{\frac{1}{2}\rho u_\infty^2} + \frac{2g(\bar{h}_1 - \bar{h}_8)}{u_\infty^2} + \frac{\overline{u_1^2}}{u_\infty^2}} \qquad (10)$$

or alternatively,

$$\frac{\bar{u}_8}{u_\infty} = \pm\sqrt{\overline{C_{p_1}} + \Delta C_p + \frac{2}{Fn^2}\cdot\frac{(\bar{h}_1 - \bar{h}_8)}{L_{pp}} + \frac{\overline{u_1^2}}{u_\infty^2}} \qquad (11)$$

where $L_{pp}$is the length between perpendiculars and Fn is the Froude number of the craft.

$$Fn = \frac{u_\infty}{\sqrt{g \cdot L_{pp}}} \qquad (12)$$

In the literature $\bar{u}_8/u_\infty$is called the Nozzle Velocity Ratio, NVR, but since in the pressure jump method it is assumed that the pressure at the nozzle discharge section is atmospheric this velocity ratio can be called Jet velocity ratio, JVR, as well. If the jet contracts behind the nozzle, section 8 should really be located at the minimum jet cross section (vena contracta) but the difference is generally small.

2.3. NUMERICAL SIMULATION

The potential flow is computed using SHIPFLOW [5], a suite of computer codes based on in-house research. The XPAN module is a potential flow panel method, using Rankine sources on the hull and part of the free surface. A Neumann boundary condition for the potential is applied on the hull (corresponding to zero normal velocity) and a combined kinematic and dynamic condition is applied on the free surface at its exact location. The latter is obtained iteratively. The frictional resistance of the hull is computed by the boundary layer module XBOUND in SHIPFLOW based on the computed pressure.

To increase the accuracy of the wave resistance prediction the XPAN computation is corrected. The correction is accomplished through the formulas introduced by Höglund [6], and similar to those suggested by Harris and Schulze [7]. This method assumes that the computed skin friction is close to the values measured so that the correction can be applied only to the wave making resistance of the hull obtained from pressure integration.

Note that no pump force is used in the SHIPFLOW solution. The key is to adjust the exit velocity, $\bar{u}_8$, such that Equations (8) and (11) are satisfied simultaneously. This has to be done iteratively. After each iteration, all terms on the right hand side of Equation (8) are known, which means that the total resistance can be computed and inserted into Equation (8) to obtain Δp. This is then inserted (non-dimensionalized) into Equation (11), where $\overline{C_{p_1}}$ is obtained as the potential flow pressure on the hull at point A and u_1^2 is taken as the average of the squared velocity at the capture area, considering the boundary layer velocity profile computed by XBOUND. A new $\bar{u}_8$ can then be obtained and the process repeated. Since the self-propelled hull resistance is not known in the first iteration, it is convenient to start the process by employing the bare hull resistance instead.

To account for the trimming moment due to the water jet, the position (height) of the thrust force $\Delta p \cdot A_{nozzle}$ is specified at the centre of the impeller disk along the shaft line. SHIPFLOW then automatically trims the hull to balance the moment created by the total resistance force and the thrust.

3. PRESSURE JUMP METHOD VALIDATION

Computational results obtained from the combination of potential flow simulation and the pressure jump method are presented in this section to validate the method. The hull investigated is R/V ATHENA which is selected by the ITTC Specialist Committee on Waterjets [8]. The measured data used for the validation of the pressure jump method are shown as symbols in the following plots. Each symbol represents an institute that participated in the ITTC measurement campaign [3].

Figure 4 depicts the predicted bare hull resistance and its comparison with the measurements. The original resistance curve from the potential flow simulation, the solid line, under-predicts the actual resistance of the bare hull in most of the Froude number range. The corrected resistance curve, represented by the dashed line, shows a better correlation with the measurement.

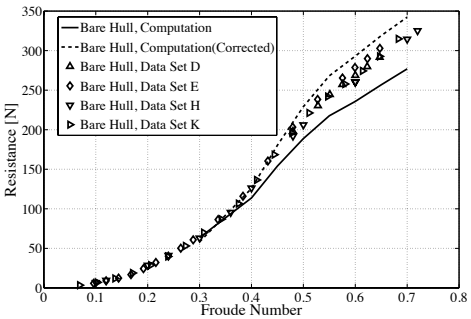

Figure 4. Resistance of the bare hull

Figure 5 shows the variation of the trim angle for both the bare hull and the self-propelled hull against Froude number. Comparing the computed bare hull trim angle with that obtained from the measurements, it is seen that the calculated trim angle is under-predicted for Froude numbers larger than 0.45 No correction is available for the sinkage and trim.

Comparing the computed trim angles for the bare hull and the self-propelled one, they are the same for Froude numbers below 0.55. For higher Froude numbers, the trim angle of the self-propelled hull becomes slightly smaller. The reason for the lower trim angle of the self-propelled hull is the action of the waterjet system, which causes a bow down trimming moment.

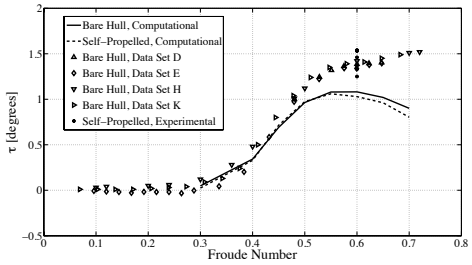

Figure 5. Trim angle versus Froude number

Figure 6 depicts the sinkage of the hull measured at half LPP. Since the vertical axis of the coordinate system is pointing upwards, the negative values for the sinkage means that the hull has moved downwards. Comparing the bare hull sinkage with the measurement good agreement is seen for Froude numbers below 0.6; but for higher Froude numbers, the computed sinkage is under-predicted. Comparing the computed self-propulsion sinkage with the measurement is a bit tricky since the scatter for the measured values is large.

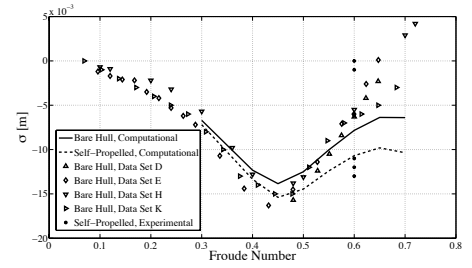

Figure 6. Sinkage at $\frac{1}{2}$LPP versus Froude number

Figure 7 shows both total thrust deduction fraction t and resistance increment fraction, t_r (Equation (5)). Experimental data are shown for the total thrust deduction fraction. Like in previous plots the total thrust deduction fraction is within the experimental scatter. The measured thrust deduction fraction plotted in this figure is obtained from the measured model scale bare hull resistance and gross thrust.

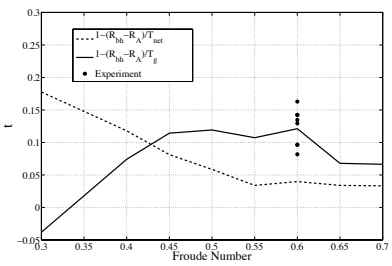

Figure 7. Thrust deduction fraction

4. A FLOW CHART OF CONTRIBUTIONS TO THE THRUST DEDUCTION

Since the objective of the present paper is to study the physics behind the waterjet-hull interaction and the corresponding thrust deduction, the possible parameters linking the bare hull resistance to the gross thrust of the self-propelled hull are identified in this Section. These two items appear on the top and bottom of the flowchart of Figure 8. All other items appearing in-between contribute to the total thrust deduction fraction.

The flowchart can be split into two major parts; the part connecting the bare hull resistance to the net thrust and the part relating the net thrust to the gross thrust. These parts define the thrust deduction fractions t_r and t_j respectively.

As seen in Figure 8 the difference between the bare hull resistance and the self-propelled hull resistance is caused by three effects, the changes of sinkage, trim and flow around the intake. The combined effect of sinkage and trim can be called global flow pattern change and the contribution of the flow change around the intake can be referred to as local flow change. Assuming that sinkage, trim and the local flow changes independently influence the resistance change, the resistance increment of the hull may be estimated from a linear expansion in a Taylor series and expressed as follows [1].

$$\Delta R(Q, d\sigma, d\tau) = \frac{\partial R}{\partial \sigma}(Q,0,0)d\sigma + \frac{\partial R}{\partial \tau}(Q,0,0)d\tau + \Delta R(Q,0,0) \qquad (13)$$

where, R is the hull resistance and Q, σ and τ are the flow rate through the ducting channel, the hull sinkage and the hull trim angle, respectively.

The bare hull equilibrium position is the reference point, about which the Taylor expansion is made. Obtaining the partial derivatives of resistance with respect to sinkage, trim and flow rate individually, the contribution of each of them to the resistance increment may be estimated.

At full scale the self-propelled hull resistance is equal to the net thrust, but at model scale a towing force, called rope force, is applied to the self-propelled hull to account for the too large frictional resistance. The net thrust is thus reduced by this force, as appears Figure 8.

To further explore the influence of various parameters the sinkage, trim and local flow effects have been subdivided into different components in Figure 8. The occurrence and magnitude of these effects depends on the definition of the bare hull condition. In this investigation the bare hull case is defined as a case where the propulsor has no influence on the sinkage, trim and local flow. Thus the hull is pushed (or towed) horizontally at the height of the centre of effort of the resistance. In this way, the true effects of the propulsor on the resistance may be investigated. It should be stressed that this condition is somewhat theoretical, since neither propeller driven nor waterjet driven hulls normally satisfy these conditions. The effects of deviations from this ideal case in the bare hull testing will be discussed below.

Perhaps the most basic influence on the global effects, sinkage and trim, comes from the change in pressure distribution on the hull due to the waterjet intake, and the

most fundamental case that can reveal such an influence is that of an infinitely large horizontal flat plate with an intake. The effect is denoted “Infinite Plate” in Figure 8, and the case is referred to as “free-stream condition” in the following. In this condition there is also a duct attached to the intake ejecting the jet horizontally. It is shown in [4] that both sinkage and trim are identically zero under these conditions.

A more realistic case is obtained if only part of the infinite plate is considered. The part of the plate, with an area and beam similar to the hull in question, may be considered separately from the rest of the infinite plate, which thus represents the water surface. From the same solution as above the forces and moments on the “hull plate” can then be obtained. In the flowchart this case is referred to as “Finite Plate”.

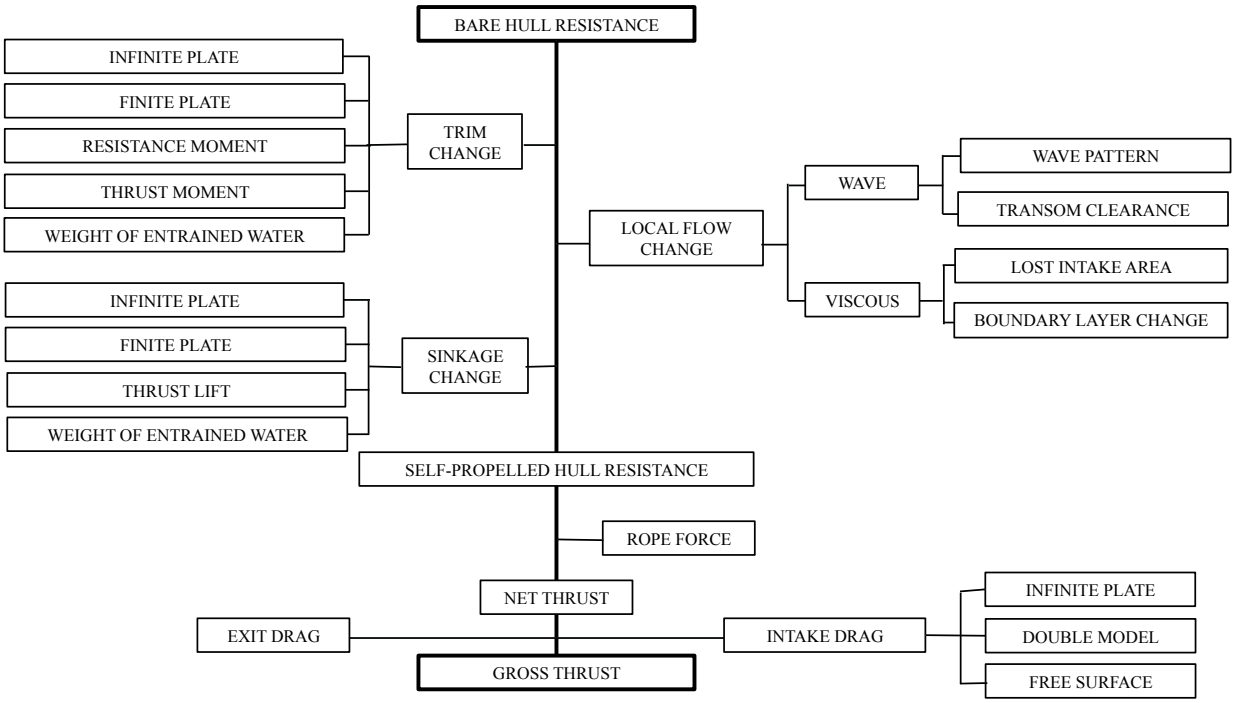

Figure 8. Contribution of different parameters on thrust deduction of a waterjet propelled craft

If the thrust is not horizontal, and not applied at the same height as the resistance, a lift force and a trimming moment are created. The lift is denoted “Thrust Lift” in the flowchart. The moment is related to the centre of floatation and split into two components the “Resistance Moment” and the “Thrust moment”, as will be further explained below.

The ducting system of the waterjet obviously contains water, not present in the bare hull case. This water will generate a vertical force and a moment on the hull thus altering the sinkage and trim. In the figure this effect is termed “Weight of Entrained Water”.

It should be noted that if the bare hull is tested according to the ITTC recommendations [9], it is towed along the pump shaft axis, and the effect of the entrained water is taken into account by an additional weight at the stern of the hull. This is to approximately account for the inclined shaft and the entrained water already in the bare hull testing. Obviously the Thrust Lift, Thrust Moment and Resistance Moment for the self-propelled hull will then be much smaller, but they will not disappear entirely. Since the resistance of the self-propelled hull differs from that of the bare hull, there will be some contribution to all three. This contribution may be called a second order quantity and its magnitude is t_r times the first order quantity, i.e. it is normally at least one order of magnitude smaller than the first order quantity.

Due to the installation of the ducting channel, as well as the ingestion of the flow into the waterjet unit, some differences in the flow field in the aft part of the hull may occur in comparison to the flow field around the bare hull. This may have some impact on the increment of the resistance of the self-propelled hull. One may split the effect into the change in wave making resistance and that in viscous resistance.

The suction of the waterjet system results in a different wave pattern next to the aft part of the hull. The free surface is sucked down, and this may have different implications if the surface has a wave crest or a wave trough at this location. This effect is indicated as “Wave Pattern” in the flow chart.

As will be seen below, the suction of the water jet has several effects on the critical Froude number, where the transom clears the water. These effects may be quite important for the thrust deduction, particularly in the Froude number range where the transom is dry for the self-propelled hull, but not for the bare hull. Effects of this kind are denoted “Transom Clearance” in the flow chart.

There are also some changes in the viscous flow around the hull. One may relate these viscous flow changes partly to the missing area of the bare hull surface, at the intake opening and partly to the boundary layer change in the vicinity of the intake due to the suction.
In the lower part of Figure 8 the effects relating net thrust and gross thrust are displayed. One component is the "Exit Drag" which occurs whenever the jet exit is submerged, or partly submerged, into the flow behind the transom. This situation occurs at low speeds, either when the water does not clear the transom or when the protruding part of the nozzle hits the (steep) stern wave.
Intake Drag is related to the forces on the protruding part of the control volume used in the momentum balance for obtaining gross thrust (See Figure 1). As will be seen below, this effect is zero under free-stream conditions, but not for a real case. The deviations from the free-stream conditions are denoted "Double Model" and "Free Surface", respectively.

4.1. RESISTANCE INCREMENT ESTIMATION

As introduced in Section 4, the resistance increment of the hull is a function of three independent variables: the hull sinkage, the hull trim and the flow rate through the waterjet system. In the following, the magnitude of the sinkage, trim and local flow change effect on the hull resistance increment will be estimated for R/V ATHENA.
To start with, the self-propelled hull equilibrium position was set to the reference sinkage and trim obtained from the bare hull simulation. Thereafter, one of the parameters sinkage, trim or flow rate was varied while the other two were kept fixed at the reference values. This procedure was accomplished for all three parameters. In order to make the sinkage and trim variations independent, the sinkage needs to be measured at the centre of floatation (CoF), where the hull does not change its displacement due to trimming. Going through this procedure provides three curves for resistance variations depending on variations of the sinkage, trim and flow rate. The curves obtained for R/V ATHENA are shown in Figure 9, Figure 10 and Figure 11, respectively. The effect of the flow rate variation on the resistance change is studied by NVR variations. Since the variation of the parameters is accomplished for discrete points, the derivatives were obtained through a curve fit.
Obviously, increasing the hull sinkage increases the total resistance of the hull (see Figure 9) but this is not necessarily the case for the trim angle (see Figure 10). The trim angle variation reveals that there is an optimum trim angle for the hull and depending on the bare hull trim angle, as well as the bow down or bow up trimming moment (most probably bow down) created by the waterjet system, the hull resistance may increase or decrease in self-propulsion.
The optimum trim angle for a hull is closely related to the optimum transom area of the hull. As mentioned by Larsson and Raven [10], there is an optimum transom area for transom-stern hull types which increases with speed. According to the optimum values of the optimum transom area, one may investigate whether the waterjet system trimming moment and sinking force helps to approach the optimum value or cause the transom area to move away from the optimum value. The last term of Equation (13) shows the impact of local flow change on the resistance increment. As seen in Figure 11. Resistance versus NVR for ATHENA at Fn=0.6. the hull resistance is almost independent of the flow rate and the slope of the curve is almost zero.

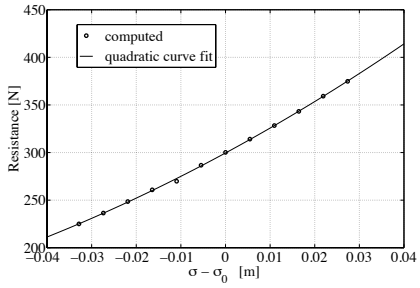

Figure 9. Resistance versus sinkage for ATHENA at Fn=0.6.

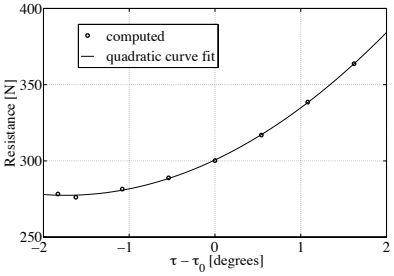

Figure 10. Resistance versus trim for ATHENA at Fn=0.6.

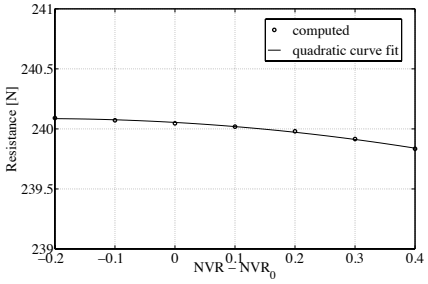

Figure 11. Resistance versus NVR for ATHENA at Fn=0.6.

With the derivatives of the resistance at hand, one may obtain the contribution of the terms in Equation (13). For this purpose, the derivatives of resistance with respect to sinkage and trim can be obtained from the curves provided in Figure 9 and Figure 10 at the point where the sinkage and trim of the self-propelled hull is the same as the bare hull. Then, multiplying these derivatives by the actual sinkage and trim change between the self-propelled hull and the bare hull (Figure 6 and Figure 5), the contribution of sinkage and trim to the resistance increment is obtained. The values of the resistance increment due to sinkage and trim for the R/V ATHENA hull at Fn=0.6 are given in Table 1.

As mentioned earlier, one can split the effect of the local flow change into wave making and viscous resistance. Table 1 shows the components of the local flow change, which contribute to the resistance increment. The wave making resistance is split into two components, where the first one is due to the change in wave pattern. It is seen that the wave trough is becoming deeper due to the suction. The second component is the effect on the transom clearance. Since the Froude number 0.6 for Athena is well above the critical value there is no effect of the difference in critical values between the bare hull and the self-propelled hull. There might be an effect of the interaction between the jet and the wave, but even this is unlikely at this relatively high Froude number for ATHENA. The value for his component is likely to be negligible, but it is marked as not estimated.

Table 1. Resistance increment (Newton) due to the sinkage and trim and local flow change and its components

<table>
<tr><td>Trim change</td><td colspan="4">$\frac{\partial R}{\partial \tau}(Q,0,0)d\tau$: -0.1</td></tr>
<tr><td>Sinkage change</td><td colspan="4">$\frac{\partial R}{\partial \sigma}(Q,0,0)d\sigma$: $+7.8$</td></tr>
<tr><td>Local flow change</td><td colspan="4">$\Delta R(Q,0,0))$: +1.6</td></tr>
<tr><td></td><td colspan="2">Wave making resistance: +9.3</td><td colspan="2">Viscous resistance: -7.7</td></tr>
<tr><td></td><td>Wave pattern: +9.3</td><td>Transom clearance: not estimated</td><td>Missing intake area: -7.2</td><td>Boundary layer change: not estimated</td></tr>
</table>

The viscous resistance change due to the local flow change is obtained by comparing the viscous resistance of the hull with or without intake. The missing surface at the intake opening for the hull with the ducting channel, results in a smaller viscous resistance, and as can be seen in the table this reduction accounts for almost the entire viscous resistance drop. The contribution from the changed boundary layer should thus be very small. It has not been estimated in the present work, but this should be done in further work. In general, one may conclude that there is some minor change in the wave making resistance and viscous resistance of the hull caused by the local flow change. These components are of the same order but have different signs. Consequently, they almost cancel each other and the total effect of the local flow change on the resistance increment becomes very small.

Concluding the results given in Table 1, the total resistance increment of the hull is obtained as follows:

$$\Delta R_{est}(Q,d\sigma,d\tau) = \frac{\partial R}{\partial \sigma}(Q,0,0)d\sigma + \frac{\partial R}{\partial \tau}(Q,0,0)d\tau + \Delta R(Q,0,0)$$
$$= \quad +7.8 \quad -0.1 \quad +1.6 \quad = \quad 9.3 \ \text{[N]}$$

This is an estimation of the hull resistance increment and can be compared with the computed resistance increment obtained from pressure jump method, [4]. The computed bare hull and self-propelled hull resistances are 293.0 and 304.2 N, respectively, so the resistance increase is 11.2 N.

Comparing the estimated resistance increment and the computed resistance increment via pressure jump method indicates that there is a decent correspondence of the estimated ΔR with the computed one. Since the estimation of the resistance increment is based on the independency of the hull sinkage, trim and local flow changes, the difference between the obtained resistance increments might be related to non-linear relations between the three mentioned effects, but it is more likely that the numerical accuracy of the value from the direct simulation is too low. This small value is calculated by subtracting two large numbers, which reduces the numerical accuracy. But in general, the estimated resistance increment suggests that the assumption of linear relation of the hull sinkage, trim and local flow changes on the resistance increment seems reasonable. Therefore, the relative magnitudes should also be reasonable, and it may be concluded that the sinkage has by far the largest influence on the resistance for this case, followed by the influence of the local flow change.

4.2. ESTIMATION OF THE DIFFERENCE BETWEEN NET AND GROSS THRUST

The exit drag for R/V ATHENA at a Froude number of 0.6 is zero, since the jet exit is well in front of the stern wave. There may however be a significant intake drag. A direct computation based on the definition (or possibly based on the different contributions) cannot be made using the main tools of the present investigation: potential flow and boundary layer methods, but it may well be done using a viscous flow method of the RANS type. This should be done in further work.

Since a direct computation cannot be made of the intake drag, an indirect estimation can be made by comparing the computed net and gross thrusts for ATHENA using the pressure jump method. For a Froude number of 0.6 the net thrust is 280 N, while the gross thrust is 306 N. The difference is thus 26 N, or 8.5% of the gross thrust. This is a surprisingly large number, which must be treated with caution. Again, we have a difference between two large numbers obtained in completely different ways.

5. CONCLUSIONS

The Pressure Jump Method is robust and very fast and can be employed for power prediction of a waterjet-propelled hull in a range of Froude numbers. The computed sinkage and trim obtained employing this method reveal that for the case studied in this paper the force and moment created by the waterjet units cause the hull to sink deeper and trim bow down comparing to the bare hull case. It should be noted that the predicted thrust deduction fraction is positive, as well as all the measured data.

A mapping of the waterjet/hull interaction effects has been presented in the form of a flow chart. This chart includes all effects envisioned to relate bare hull resistance and gross thrust. Its main components are

sinkage, trim, local effects, intake drag and exit drag. All are discussed in the report. The sinkage, trim and local flow effects are subdivided into components, and based on an analysis of these components the following conclusions may be drawn:

- There is no sinkage or trim for a waterjet in free-stream conditions, i.e. for a waterjet fitted to an infinitely large flat plate and ejecting the flow horizontally. This is under the condition of infinitely deep water.
- The waterjet induced pressure on the hull increases the sinkage, which increases resistance.
- For most hulls the waterjet system generates a bow-down trimming moment but depending on the position of the waterjet unit the trimming moment might be bow-up.
- An inclination of the waterjet nozzle always induces a bow-down effect, as does the resistance/thrust couple.
- There is an optimum trim angle for the hull where the resistance is minimum. This is normally obtained where the transom has an optimum size. An increased trim may increase or decrease the resistance depending on the position on the resistance/trim curve relative to the optimum trim angle. The trim angle is one candidate for reducing the resistance, unless the hull has been optimized for self-propulsion.
- Wave resistance normally increases due to deepening of wave trough at the stern.
- The viscous resistance decreases due to the missing surface covering the intake opening, but it may increase somewhat due to the changes in the boundary layer around the intake.

6. ACKNOWLEDGEMENTS

The research has been sponsored by Rolls-Royce Marine through the University Technology Centre at Chalmers.

7. REFERENCES

- T. van Terwisga, “Waterjet-Hull Interaction”, PhD thesis, *Delft Technical University*, 1996.
- “*The Specialist Committee on Validation of Waterjet Test Procedures Final Report and Recommendations to the 24th ITTC*” vol. II, pp. 471–508, 2004.
- “*The Specialist Committee on Validation of Waterjet Test Procedures, Proceedings of the 24th ITTC*” 2005.
- A. Eslamdoost, “Investigations of Waterjet/Hull Interaction Effects”, Licentiate thesis, *Chalmers University of Technology*, 2012.
- “SHIPFLOW” *FLOWTECH AB*, Gothenburg.
- V. Höglund, “Validation and Correction of SHIPFLOW for Fast Hulls”, MSc thesis, *Chalmers University of Technology*, 2004.
- S. Harries and D. Schulze, “Numerical investigation of a systematic model series for the design of fast monohulls”, in *International Conference on Fast Sea Transportation, FAST ’97*, 1997.
- “*The Specialist Committee on Validation of Waterjet Test Procedures: Final Report and Recommendations to the 23rd ITTC*”, 2002.
- “ITTC Recommended Procedures and Guidelines; Waterjet Propulsive Performance Prediction”, *International Towing Tank Conference*, 2004.
- L. Larsson and H. C. Raven, "Ship resistance and flow", *The Society of Naval Architects and Marine Engineers*, 2010.